Available online at www.sciencedirect.com
ScienceDirect
Applied Surface Science 254 (2008) 2905–2910
applied surface science
www.elsevier.com/locate/apsusc

Surface evolution of a gradient structured Ti in hydrogen peroxide solution

Ming Wen [a,b], Jian-Feng Gu [a,*], Gang Liu [b], Zhen-Bo Wang [b], Jian Lu [c]

[a] School of Materials Science and Engineering, Shanghai Jiao Tong University, Shanghai 200240, People's Republic of China
[b] Shenyang National Laboratory for Materials Science, Institute of Metals Research, Chinese Academy of Sciences, Shenyang 110016, People's Republic of China
[c] Mechanical Engineering Department, The Hong Kong Polytechnic University, Hong Kong, People's Republic of China

Received 30 May 2007; received in revised form 15 October 2007; accepted 15 October 2007
Available online 22 October 2007

Abstract

In this work, the interaction between hydrogen peroxide (H_2O_2) and a gradient structured Ti was investigated extensively. The gradient structured Ti (SMAT Ti) was produced by surface mechanical attrition treatment (SMAT), and then it was immersed in H_2O_2 solution for different time until 48 h at room temperature (25 °C). The structure and surface morphology evolution were examined by Raman spectra and scanning electron microscopy (SEM). The formation mechanism of nanoporous titania was discussed based on above results.

PACS : 61.46.HK; 68.35.BS

Keywords: Gradient structure; Titanium; Nanoporous; titania

1. Introduction

Titanium and its alloys are frequently employed for dental and orthopedic implants due to the low toxicity, low corrosion rate, favorable mechanical properties, and good biocompatibility [1,2]. Upon implantation, the implant surface is conditioned by proteins, ions, sugars, and lipids present in the blood and tissue fluids. The important surface properties affecting this process include topography, chemistry, surface charge, and hydrophilicity [3]. A key issue in most application of biomaterials is how the material influences, and is influenced by the biological response resulting from the contact between the biomaterial and the biological system. Until now, the understanding about this field is still very limited [4]. Hydrogen peroxide (H_2O_2) is an important oxidizing component for wound healing, which may be produced in the body through the following ways: molecular oxygen is firstly reduced to a highly reactive and unstable superoxide anion radical (O_2^-), and superoxide dismutase (SOD), produced by inflammatory cells, further catalyze O_2^- doubly protonated in the body to form H_2O_2. The reaction can be expressed as [5–7]:

$$O_2^- + O_2^- + 2H^+ \xrightarrow{SOD} H_2O_2 + O_2 \quad (1)$$

So it is important to investigate the interaction between implant and H_2O_2. In the case of titanium, it is very interesting to find that there are few hydroxyl radicals (potent agents for cellular deterioration) formed from the interaction with H_2O_2. Tengvall et al. suggested that it could be attributed to the quenching of Fenton reaction through both trapping and oxidation of superoxide radicals in a TiOOH matrix [6]. Pan et al. found that a decreased corrosion resistance and consequently an oxide film thickening phenomenon happened when Ti was immersed in a phosphate-buffered saline (PBS) solution with H_2O_2 addition, and the film could be described by a two-layer model with a barrier inner layer and porous outer layer [7,8]. Though they did not describe the size of the pore, H_2O_2 addition seemed to facilitate the incorporation of ions into the thicker porous layer, thus favored the precipitation of hydroxylcarbonated apatite (HCA) during the cell culture [9].

All above used Ti plates were coarse-grained (CG). At the same time, nanostructured metals exhibiting unique physical, chemical and mechanical properties have attracted tremendous

* Corresponding author. Tel.: +8621 34203743; fax: +8621 34203742.
E-mail address: Gujf@sjtu.edu.cn (J.-F. Gu).

0169-4332/$ – see front matter © 2007 Elsevier B.V. All rights reserved.
doi:10.1016/j.apsusc.2007.10.035

attention in recent years, and it is important to identify and exploit the unique, superior properties and the new applications of these novel materials [10]. Until now, the usual method to refine grain size of bulk metal is severe plastic deformation (SPD), which includes equal-channel angular pressing (ECAP), high-pressure torsion (HPT), and repeated cold-rolling [11]. However, the grain size of Ti can only achieve 200–300 nm by ECAP and it is even over than 100 nm by cold-rolling, HPT, or cold extrusion following ECAP [12–14]. At the same time, it is well known that most failures of materials occur on surfaces, including fatigue fracture, fretting fatigue, wear and corrosion, etc., which are very sensitive to the structure and properties of the material surface. Optimization of the surface structure of materials is of great importance to the global behavior of a material. The newly developed surface mechanical attrition treatment (SMAT), introducing a large amount of defects and/or interfaces into the surface layer so that its microstructure is transformed into nano-sized crystallites, is an effective way to realize surface self-nanocrystallization on metallic materials without changing the chemical compositions, and it is has been used successfully in Fe, Cu, and stainless steel, etc. [15,16]. In the SMAT materials, the grain size increase gradually with no obvious interfaces from top-surface to matrix, and it is a very promising method to produce functionally gradient materials since the nanostructured surface provides the much improved properties (such as high strength, wear resistance and chemical reactivity, etc.) while the CG matrix supplies the ductility.

In the last work [17], we reported that the phenomena of nanoporous titania produced by hybrid SMAT showed high thermal stability. As a continuation of the previous work to investigate the formation mechanism of nanoporous titania, we further studied the details of: (1) the gradient structure of SMAT Ti; (2) the structure and surface morphology evolution of SMAT Ti while it was immersed in H_2O_2 solution for different time at room temperature.

2. Experimental

The material used in this study was a Ti plate with the chemical composition (wt%): 0.10 Fe, 0.01 Si, 0.16 O, 0.014 N, 0.004 H, 0.022 C, 0.23 Al and balance Ti. The plate was annealed in argon atmosphere at 740 °C for 2 h, and then air-cooled, resulting in equiaxed grains averaging 30 μm in size. The SMAT set-up had been described in detail elsewhere [15,16]. In this study, the vibration frequency of the system was 50 Hz, stainless steel balls with the diameter of 8 mm were used and the samples were treated in vacuum for 60 min at room temperature. The cross-section observations of SMAT Ti were performed by a Leica MPS30 optical microscope. TEM images and the corresponding selected area electron diffraction (SAED) were obtained by using a JEOL 2010 TEM with an accelerating voltage of 200 kV. The TEM specimen of top-surface was prepared by means of polishing, dimpling and ion thinning only from the untreated side at low temperature. The TEM specimens of different layers were obtained by polishing the corresponding layer, then mechanically thinned from the untreated side until the thickness was about 30 μm, and followed by a twin jet-polishing with an electrolyte consisting of 30 ml perchloric acid, 175 ml butyl alcohol and 300 ml methanol at a temperature of −30 °C. Then the SMAT Ti plates were immersed in 30 wt% H_2O_2 for different time until 48 h at room temperature. After that, the plate was rinsed with distilled water and dried at 40 °C for 6 h. For comparison, a CG Ti was also prepared according to the same procedure only in the absence of SMAT. The phase constitutions of the as-prepared samples surface were characterized by the Raman spectra (Jobin Yvon HR800, 632.8 nm laser). Field emission scanning electron microscopy (FSEM: Supra 35 LEΦ FSEM) analyses were conducted to examine the surface morphology.

3. Results and discussion

3.1. The gradient structure of Ti subjected SMAT only

Fig. 1 is the cross-sectional optical microstructures of the SMAT Ti sample. It is obvious that the treated surface layer is much blacker than that in the matrix. The sample can accordingly be subdivided into three regions: (1) the severe deformation layers (about 150–200 μm) in which the grain boundaries could not be identified; (2) minor deformation layers in which mechanical twins and their interactions are visible next to the severe deformation layers; and (3) strain-free matrix. Due to limited resolving power of the optical microscopy, TEM was used to investigate the structures in the severe deformation layers.

Fig. 2 shows the typical plane-view TEM observations of the top surface layer and layers at different depths from the treated surface. A typical dark field image of the SMAT sample (before oxidation) top-surface is presented in Fig. 2a. It is characterized by wavy-like and irregular grains with a large number of dislocations, and the corresponding selected area electron diffraction (SAED) suggests the existence of both large and low angle grain boundaries. The average grain size is about 30 nm measured from a number of TEM images. The dark field TEM image and the corresponding SAED of SMAT Ti at about 60 μm below top-surface are shown in Fig. 2b. As compared

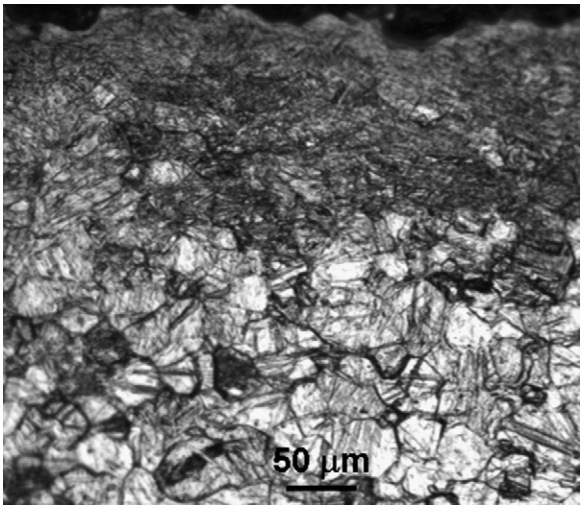

Fig. 1. A cross-sectional optical micrograph of the SMAT Ti.

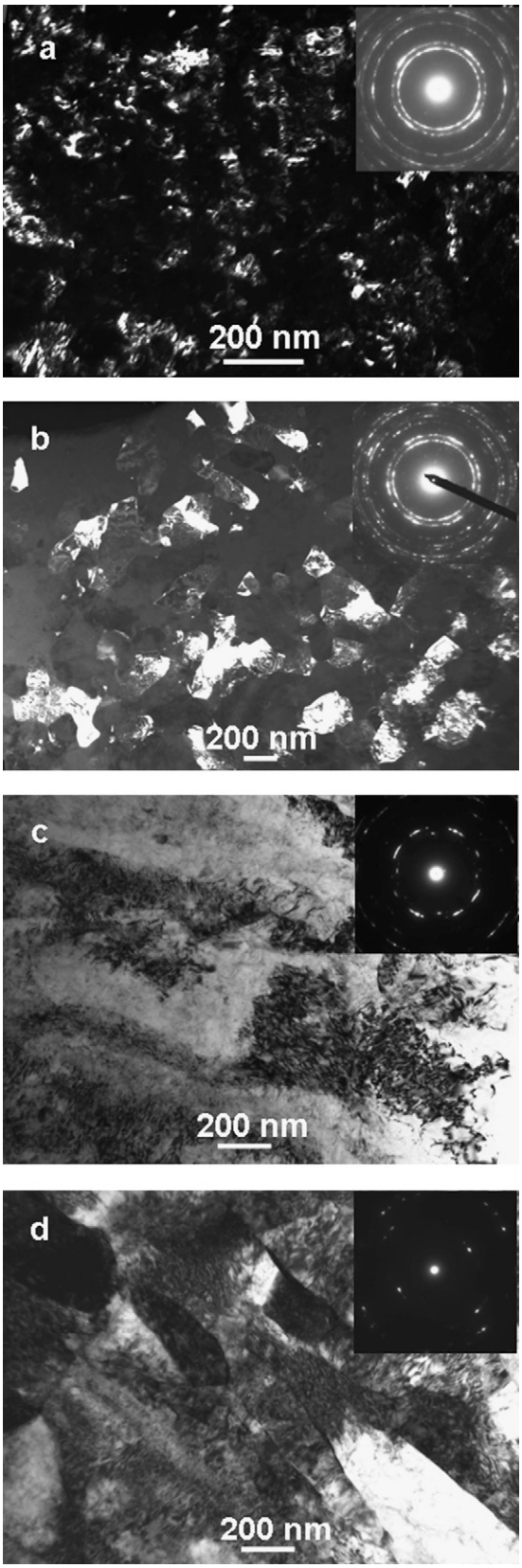

Fig. 2. Typical plane-view TEM observations and corresponding SAED of the: (a) top-surface; (b) sub-surface layer of 60 μm depth; (c) sub-surface layer of 100 μm depth; and (d) sub-surface layer of 150 μm depth in the SMAT Ti.

with Fig. 2a, the grains become larger, and the ring pattern is obviously not so consecutive. The average grain size is about 250 nm by number-averaging the diameters of 180 grains. When the depth achieves 100 μm, it is obvious that the microstructure is composed by dislocations cells which are wavy-like and irregular, and the clustered diffraction spots as well as some small arcs suggest that the grain boundaries are mostly low angle type (Fig. 2c). The low angle grain boundaries were caused by the relatively small strain and strain rate at the current depth. Fig. 2d shows the bright field image of SMAT Ti at the depth of 150 μm. The reorientation bands (RBS) were found in this depth and the dislocations distribution are not uniform even in the band interior. The corresponding SEAD shows undeveloped arcs with well-defined diffraction spots suggesting that the RBS are low angle misorientations.

The above results clearly illustrate that a nanostructured surface layer was developed in the SMAT Ti. The grain size increased and the grain orientations became less random with the increasing distance from top-surface; in other word; a gradient structured Ti was formed after SMAT.

3.2. The structure and surface morphology evolution of Ti in H_2O_2

Fig. 3 shows the Raman spectra of coarse-grained Ti (a) and SMAT Ti (b) immersed in H_2O_2 solution for different time. There is no band in the Raman spectra of CG Ti from 4 to 48 h (Fig. 3a), which suggests the poor oxidation and crystallization capability of the Ti gel formed on the surface. As for the SMAT Ti (Fig. 3b), there is also no band in sample both before immersion and after 4 h in H_2O_2. A weak band at 156 cm^{-1} which can be assigned to E_g of anatase appears after 12 h, showing the beginning crystallization state of anatase. With even longer immersion time over 12 h, the band becomes stronger and reaches the peak value after 24 h. But it vanishes again after 36 h, and it can be inferred to the dissolution of crystalline anatase at this stage. From above discussion, it is believed that the crystallization time of anatase in H_2O_2 solution is between 4 and 12 h.

Fig. 4 shows the SEM images of CG Ti after immersing in H_2O_2 for different time. It is very clear that intergranular corrosion appears only after 4 h (Fig. 4a), which is caused by the higher chemical reactivity of grain boundary than that of the grain interior. In the same time, some pores with the size about 1–2 μm appear in the grain interior. The width of groove formed in grain boundary is about 0.3 μm after 4 h, and it becomes wider and wider with time which can be seen clearly in Fig. 4a–c. After 24 h, some of the surface grains begin dissolving in the solution (Fig. 4d), and the grain in the sub-surface is also exposed when the time reaches 36 h (Fig. 4e). More and more sub-surface grains are exposed after 48 h, and the groove become irregular (Fig. 4f). In the case of SMAT Ti, the surface morphology evolution is obviously different compared with CG Ti. There is no obvious change after 4 h (Fig. 5a). But after 12 h, some cracks appear on the surface (Fig. 5b). Cracks become wider and longer after 20 h and some cracks even evolve into grooves, and higher magnificationin-

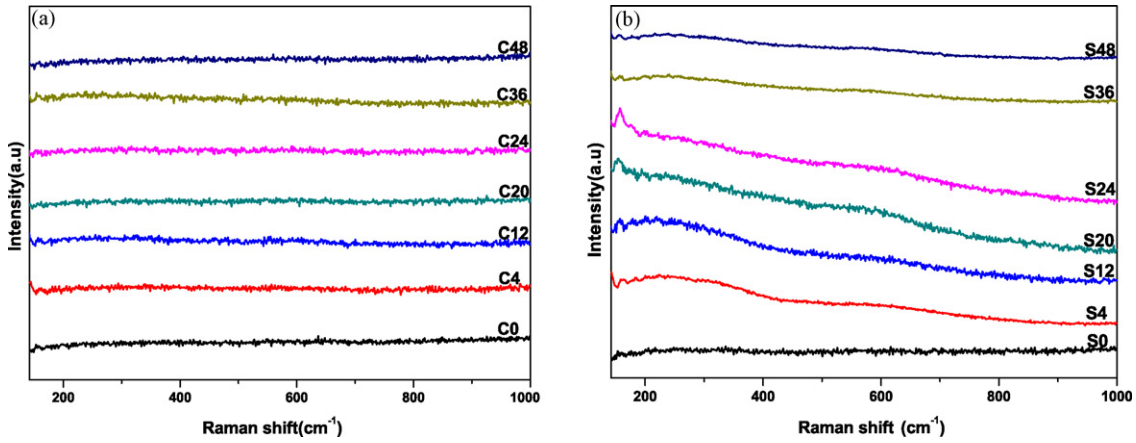

Fig. 3. Raman spectra of coarse-grained Ti (a) and SMAT Ti (b) after immersed in H_2O_2 for different time at room temperature (C: coarse-grained; S: SMAT; the number behind C or S is the immersion time).

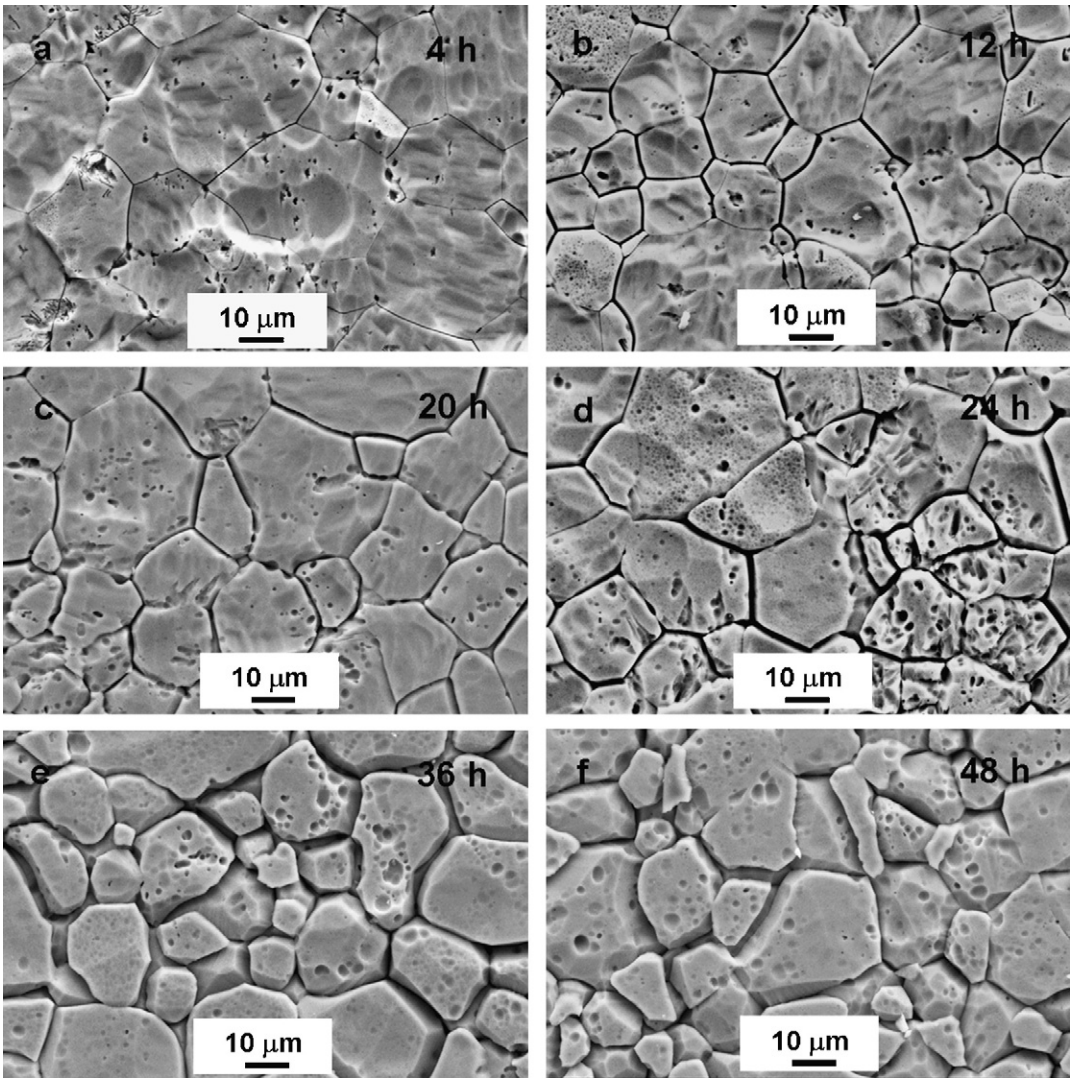

Fig. 4. SEM images of coarse-grained Ti surface after immersed in H_2O_2 for different time at room temperature (the number in the up right of the figure is the immersion time).

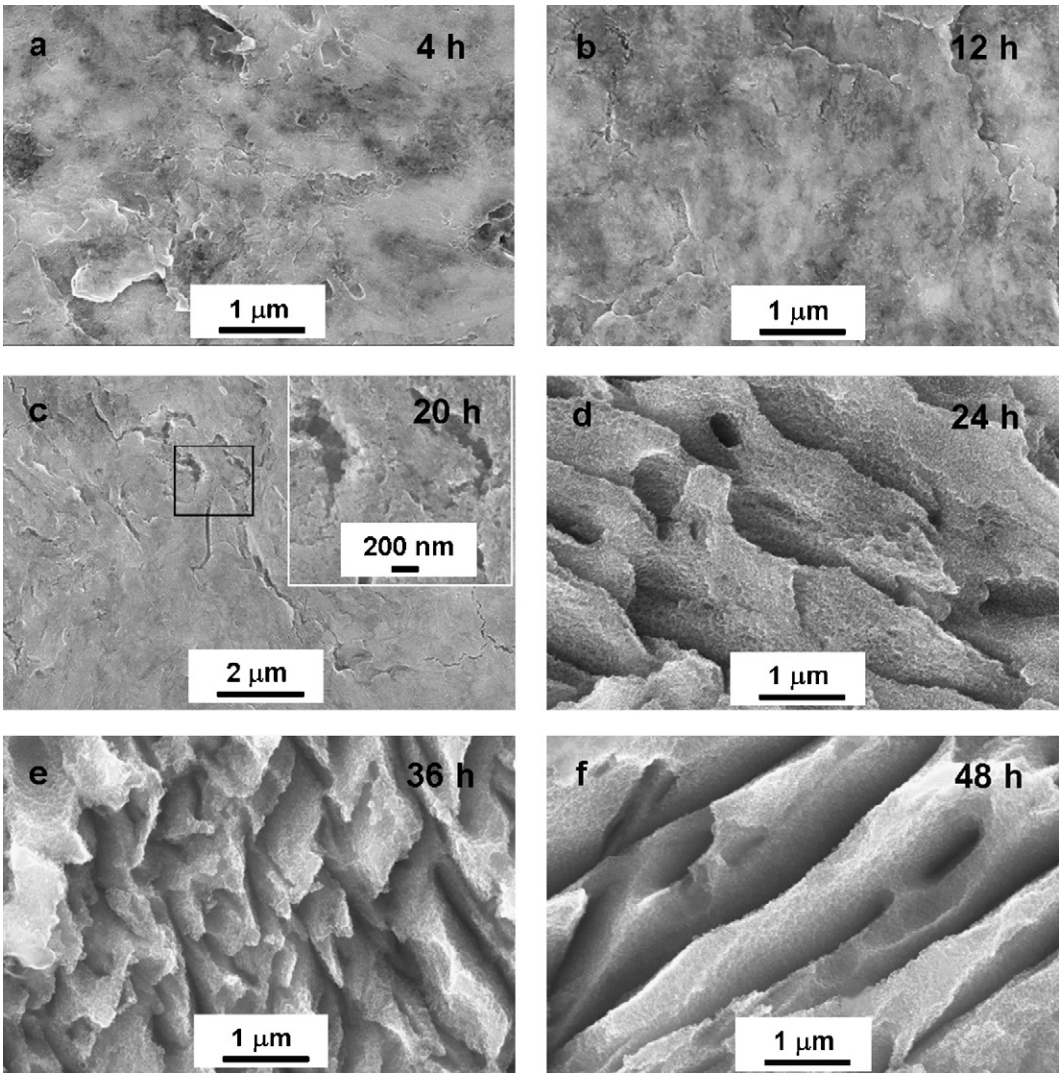

Fig. 5. SEM images of SMAT Ti surface after immersed in H_2O_2 for different time at room temperature (the number in the up right of the figure is the immersion time).

serted shows there are many small pores in the nanometer scale appearing around the grooves (Fig. 5c). After 24 h, drastic change occurs with flakes and cones covering most of the surface, and the flakes and cones are besprinkled with very small hole in the nanometer scale (Fig. 5d). The nanoporous structure can be retained even after 36 h (Fig. 5e) and 48 h (Fig. 5f).

3.3. The formation mechanism of nanoporous oxide on SMAT Ti surface

It is very interesting to find that the surface nanocrystalline Ti by SMAT can transform into nanoporous anatase by present treatment. H_2O_2 decomposition on metal surfaces (S) is suggested to proceed through the following reactions [18]:

$$\mathrm{Ti(s)} + 2\mathrm{H_2O_2} \rightarrow \mathrm{TiOOH(aq)} + 1/2\mathrm{O_2(g)} + \mathrm{H_3O^+} \quad (1)$$

$$\mathrm{TiOOH(aq)} + 1/2\mathrm{O_2(g)} + \mathrm{H_3O^+} \rightarrow \mathrm{Ti(OH)_4} \quad (2)$$

$$\mathrm{Ti(OH)_4} \rightarrow \mathrm{TiO_2(aq)} + 2\mathrm{H_2O} \quad (3)$$

$$\mathrm{Ti(OH)_4} \rightarrow \mathrm{Ti(OH)_{4-n}^{n+}} + n\mathrm{OH^-} \quad (4)$$

$$\mathrm{TiO_2(aq)} + 4\mathrm{H^+} \rightarrow \mathrm{Ti(IV)(aq)} + 2\mathrm{H_2O} \quad (5)$$

Generally, the reactions between the titanium and H_2O_2 can be interpreted by three procedures: the oxidation of titanium, titania gel formation, and Ti ion dissolution during the decomposition of H_2O_2 to O_2 and H_2O. Since dense defects such as dislocations, vacancies and a large volume fraction of grain boundaries with a high excess stored energy were observed in the nanocrystalline Ti layer after SMAT, the decomposition of H_2O_2 generating oxygen molecules, the diffusion of oxygen, and the formation of titania will preferentially occur at the sites with high energy, such as the grain boundaries and the sites with high defects density in grain interior. The titania thus formed evolves simultaneously: (1) the dissolution of titania by H_2O_2. More and more pits are left in situ in this process, and they aggregate with each other, which causes the perfect nanoporous structure come into being; (2) in situ crystallization of the amorphous titania gel. The high chemical reactivity of the nanocrystalline and dense non-equilibrium defects bring an

extra driving force stored in the SMAT Ti surface, which makes possible that the amorphous titania partly transforms to titania with weak crystallinity. In addition, the aqueous hydrogen peroxide environment may also improve the diffusivity of atoms, the nucleation and growth of crystalline phases [19], and the same procedures have been found in the nirtiding and chromizing iron or steel at low temperature [20,21].

Based on the results of Raman and SEM, the oxidation behaviors of SMAT Ti in H_2O_2 solution can be approximately depicted. At first, due to the high chemical reactivity of nanocrystalline layer on the SMAT Ti surface, it reacted with H_2O_2 quickly including the catalytic decomposition of H_2O_2 and the formation of titania [5]. Then, the titania formed began to dessolve in the solution accompanied with the in situ crystallization procedure, and thus a perfect nanoporous anatase formed. Finally, as most of the nanocrystalline Ti consumed in the solution, the oxidation and dissolution rate would slower for the bigger grain size and decreased defect density in the sub-surface of SMAT Ti and the in situ crystallization rate became slower as well. So it can be concluded that the gradient structure is responsible for the absence of Raman responses (Fig. 1b).

Muyco et al. have suggested that Ti-peroxy gel formed when Ti implant interacted with the hydrogen peroxide, and three possible functions of Ti-peroxy gel are: (1) reduction of the inflammatory response through the reduction of hydrogen peroxide and other reactive oxygen species; (2) creation of a favorable surface for calcium phosphate nucleation; and (3) as a transitional layer between the compliant surrounding tissue and the stiff titanium [22]. It has been found that the H_2O_2 pretreatment of titanium results in a thickened the porous oxide layer, a large amounts of surface hydroxyl groups favored ion incorporation, and the precipitation of the HCA-like compound on the surface during the cell culture [9]. As concerned with the nanoporous structure in the SMAT Ti, the SMAT method seems to be a possible route to improve the bioactivity of titanium bone implants and to accelerate osseointegration. Further in vivo bioactive experiments of the SMAT Ti are being conducted in our group now and will be published in the future.

4. Conclusions

In conclusion, a gradient structured Ti was formed by means of SMAT. The SMAT Ti shows much improved oxidation kinetics in H_2O_2 solution as compared with CG Ti. The formation of nanoporous structure on SMAT Ti surface can be attributed to the quick H_2O_2 decomposition, preferred oxidation of nanocrystalline Ti with dense defects to form amorphous titania, and the in situ crystallization and dissolution of titania gel. The SMAT method may be a possible route to improve the bioactivity of titanium bone implants and to accelerate osseointegration.

Acknowledgements

This work was supported by NSFC (Grant No. 50431010) and most of China (Grant No.2005CB623604) and the Hong Kong Polytechnic University (Grant No. BB90).

References

[1] T. Kokubo, H.M. Kim, M. Kawashita, T. Nakamura, J. Mater. Sci. Mater. Med. 15 (2004) 99.
[2] X.Y. Liu, P.K. Chu, C.X. Ding, Mater. Sci. Eng. R 47 (2004) 49.
[3] G. Zhao, Z. Schwartz, M. Wieland, F. Rupp, J. Geis-Gerstorfer, D.L. Cochran, B.D. boyan, J. Biomed. Mater. Res. 74 A (2005) 49.
[4] J. Lausmaa, J. Electron Spectrosc. Related Phenom. 81 (1996) 343.
[5] J.P. Bearinger, C.A. Orme, J.L. Gilbert, J. Biomed. Mater. Res. 67A (2003) 702.
[6] P. Tengvall, I. Lundstrom, L. Sjoqvist, H. Elwing, L.M. Bjursten, Biomaterials 10 (1989) 166.
[7] J. Pan, D. Thierry, C. Leygraf, J. Biomed. Mater. Res. 28 (1994) 113.
[8] J. Pan, D. Thierry, C. Leygraf, J. Biomed. Mater. Res. 30 (1996) 393.
[9] J. Pan, D. Thierry, C. Leygraf, J. Li, J. Biomed. Mater. Res. 40 (1998) 244.
[10] L. Lu, M.L. Sui, K. Lu, Science 287 (2000) 1463.
[11] R.Z. Valiev, R.K. Islamgaliev, I.V. Alexandrov, Prog. Mater. Sci. 45 (2000) 103.
[12] Y.T. Zhu, J.Y. Huang, J. Gubicza, T. Unágr, Y.M. Wang, E. Ma, R.Z. Valiev, J. Mater. Res. 18 (20031908).
[13] V.V. Stolyarov, Y.T. Zhu, T.C. Lowe, R.K. Islamgaliev, R.Z. Valiev, Nanostruc. Mater. 7 (1999) 947.
[14] V.V. Stolyarov, Y.T. Zhu, T.C. Lowe, R.Z. Valiev, Mater. Sci. Eng. A 303 (2001) 82.
[15] K. Lu, J. Lu, J. Mater. Sci. Technol. 15 (1999) 193.
[16] K. Lu, J. Lu, Mater. Sci. Eng. A 375 (2004) 38.
[17] M. Wen, J.F. Gu, G. Liu, Z.B. Wang, J. Lu, Surf. Coat. Technol. 201 (2007) 6285.
[18] A. Osaka, K. Tsuru, S. Hayakawa, Phosphorous Res. Bull. 17 (2004) 130.
[19] C. Ooka, H. Yoshida, S. Takeuchi, M. Maekaw, Z. Yamada, T. Hattori, Catal. Lett. 5 (2004) 49.
[20] W.P. Tong, N.R. Tao, Z.B. Wang, J. Lu, K. Lu, Science 299 (2003) 686.
[21] Z.B. Wang, N.R. Tao, W.P. Tong, J. Lu, K. Lu, Acta Mater. 51 (2003) 4319.
[22] J.J. Muyco, J.J. Gray, T.V. Ratto, C.A. Orme, J. McKittrick, J. Frangos, Mater. Sci. Eng. C26 (2006) 1408.